Osteoblasts induce Ca^{2+} oscillation-independent NFATc1 activation during osteoclastogenesis

Yukiko Kuroda*†, Chihiro Hisatsune*†‡, Takeshi Nakamura‡§, Koichi Matsuo¶, and Katsuhiko Mikoshiba*†‖

*Division of Molecular Neurobiology, Institute of Medical Science, University of Tokyo, 4-6-1, Shirokane-dai, Minato-ku, Tokyo 108-8639, Japan; †Developmental Neurobiology, RIKEN Brain Science Institute (BSI), 2-1 Hirosawa, Wako, Saitama 351-0198, Japan; ‡Calcium Oscillation Project, ICORP-SORST, Japan Science and Technology Agency, 2-1 Hirosawa, Wako, Saitama 351-0198, Japan; and ¶Department of Microbiology and Immunology, School of Medicine, Keio University, 35 Shinanomachi, Shinjuku-ku, Tokyo 160-8582, Japan

Edited by Solomon H. Snyder, Johns Hopkins University School of Medicine, Baltimore, MD, and approved April 7, 2008 (received for review January 23, 2008)

Intercellular cross-talk between osteoblasts and osteoclasts is important for controlling bone remolding and maintenance. However, the precise molecular mechanism by which osteoblasts regulate osteoclastogenesis is still largely unknown. Here, we show that osteoblasts can induce Ca^{2+} oscillation-independent osteoclastogenesis. We found that bone marrow-derived monocyte/macrophage precursor cells (BMMs) lacking inositol 1,4,5-trisphosphate receptor type2 (IP_3R2) did not exhibit Ca^{2+} oscillation or differentiation into multinuclear osteoclasts in response to recombinant receptor activator of NF-κB ligand/macrophage colony-stimulating factor stimulation. IP_3R2 knockout BMMs, however, underwent osteoclastogenesis when they were cocultured with osteoblasts or *in vivo* in the absence of Ca^{2+} oscillation. Furthermore, we found that Ca^{2+} oscillation-independent osteoclastogenesis was insensitive to FK506, a calcineurin inhibitor. Taken together, we conclude that both Ca^{2+} oscillation/calcineurin-dependent and -independent signaling pathways contribute to NFATc1 activation, leading to efficient osteoclastogenesis *in vivo*.

differentiation | inositol 1,4,5-trisphosphate receptor (IP3R) | osteoclast | receptor activator of NF-κB ligand (RANKL) | calcium

Skeletal development requires a delicate balance between bone formation by osteoblasts and resorption by osteoclasts, and imbalances in bone remodeling cause various types of skeletal disorders (1, 2). Excessive osteoclast differentiation and activity are the primary causes of many adult skeletal diseases. Thus, investigation of the regulatory mechanisms underlying osteoclast differentiation is crucial for understanding the physiology and pathology of the skeletal system and for developing new treatments.

Among advances in understanding molecular mechanism of osteoclast differentiation from bone marrow-derived monocyte/macrophage precursor cells (BMMs), two factors have been shown to be indispensable for osteoclastogenesis. They are the receptor activator of NF-κB ligand (RANKL), which belongs to the TNF family proteins (3–6), and macrophage colony-stimulating factor (M-CSF) (7, 8). Activation of RANK, the RANKL receptor, which is expressed on BMMs, triggers the recruitment of TNF receptor-associated factor (TRAF) family proteins, such as TRAF6 (9), followed by activation of downstream signaling molecules NF-κB, JNK, Src, and c-Fos (9–13). Takayanagi *et al.* (14) have also demonstrated a crucial role for Ca^{2+} oscillation/calcineurin-dependent activation of the nuclear factor of activated T cells (NFAT) transcription factor in osteoclastogenesis. They report that RANKL induces Ca^{2+} oscillation during osteoclast differentiation, and that this oscillation is necessary for NFATc1 activation and subsequent autoamplification. NFAT activation is tightly regulated by phosphorylation, which is controlled by the Ca^{2+}-dependent phosphatase calcineurin (15–17). Therefore, defining the precise regulatory mechanism by which Ca^{2+} concentrations affect calcineurin activity is necessary for understanding osteoclastogenesis.

One important factor determining intracellular Ca^{2+} dynamics is the inositol 1,4,5-trisphosphate receptor (IP_3R), which releases Ca^{2+} from intracellular storage sites in the endoplasmic reticulum (ER). To date, three types of IP_3Rs (IP_3R1, IP_3R2, and IP_3R3) have been identified. All exhibit the basic properties of Ca^{2+} channels but differ in terms of how their activity is regulated by ATP, IP_3, Ca^{2+}, and other proteins (18, 19). Therefore, the subunit composition and expression levels of each IP_3R subtype should create spatially and temporally diverse patterns of intracellular Ca^{2+} dynamics (20, 21). In addition, Sugawara *et al.* (22) reported complete abrogation of NFAT activation in DT40 cells lacking all three IP_3R subtypes and in which no Ca^{2+} oscillation was observed after agonist stimulation. Similarly, the contribution of IP_3-induced Ca^{2+} release to NFAT-dependent transcription has also been reported in cultured hippocampal neurons (23).

Because of the importance of IP_3Rs in intracellular Ca^{2+} dynamics, we investigated the role of IP_3Rs in osteoclast differentiation using mice lacking each IP_3R subtype (24, 25). Significantly, our analysis demonstrates the existence of a Ca^{2+} oscillation/calcineurin-independent mechanism of osteoclastogenesis activated intercellularly by osteoblasts. Our findings indicate that intercellular communication between osteoclasts and osteoblasts through both the Ca^{2+} oscillation/calcineurin-dependent and -independent signaling pathways contributes to efficient osteoclastogenesis *in vivo*.

Results

IP_3R2 Is Critical for RANKL/M-CSF-Induced Ca^{2+} Oscillation and Osteoclast Differentiation. To determine which IP_3R subtype mediates osteoclast differentiation, we first examined RANKL/M-CSF-induced osteoclastogenesis using BMMs from WT mice and from mice lacking the IP_3R subtype (24, 25). After stimulation by recombinant RANKL plus M-CSF for 4 days, BMMs from WT mice differentiated into multinuclear osteoclasts positive for tartrate-resistant acid phosphatase (TRAP), an osteoclast marker (Fig. 1*A*). Interestingly, whereas BMMs lacking IP_3R1 or IP_3R3 differentiated normally into TRAP-positive multinuclear cells similar to WT BMMs, RANKL/M-CSF-induced osteoclastogenesis was severely blocked in BMMs derived from IP_3R2 or $IP_3R2/3$ KO mice (Fig. 1*A*), suggesting a critical role of IP_3R2 in osteoclastogenesis. Consistently, immunoblotting of total

Author contributions: Y.K., C.H., and K. Mikoshiba designed research; Y.K., C.H., and K. Matsuo performed research; Y.K., T.N., and K. Matsuo analyzed data; and Y.K. and C.H. wrote the paper.

The authors declare no conflict of interest.

This article is a PNAS Direct Submission.

§Deceased July 23rd, 2006.

‖To whom correspondence should be addressed. E-mail: mikosiba@brain.riken.jp.

This article contains supporting information online at www.pnas.org/cgi/content/full/0800642105/DCSupplemental.

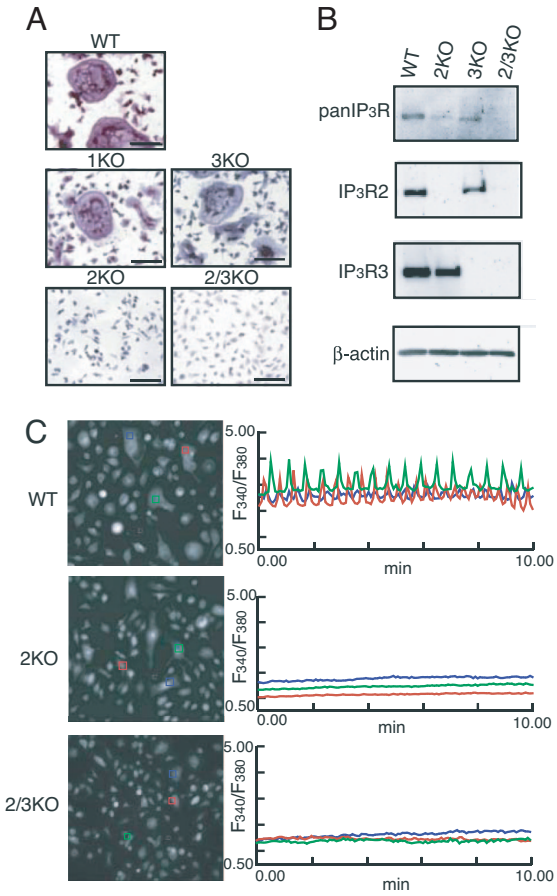

Fig. 1. Dominant expression of IP_3R2 in osteoclasts and defects in RANKL/M-CSF-induced *in vitro* osteoclastogenesis of IP_3R2-deficient BMMs. (*A*) RANKL/M-CSF-induced osteoclast formation *in vitro* (TRAP staining). (Scale bar, 50 μm.) (*B*) Expression levels of IP_3Rs. β-actin was used as an internal control. (*C*) Ca^{2+} imaging of RANKL/M-CSF-stimulated BMMs from WT, IP_3R2 KO, and $IP_3R2/3$ KO mice. *Left* show fura-2 images of recorded cells, and *Right* show traces of change in the fura-2 fluorescence ratio in single cells treated with RANKL for 48–72 h. Each colored box represents the area from which the time-course plot was calculated. All experiments were performed at least three times, and representative data are shown.

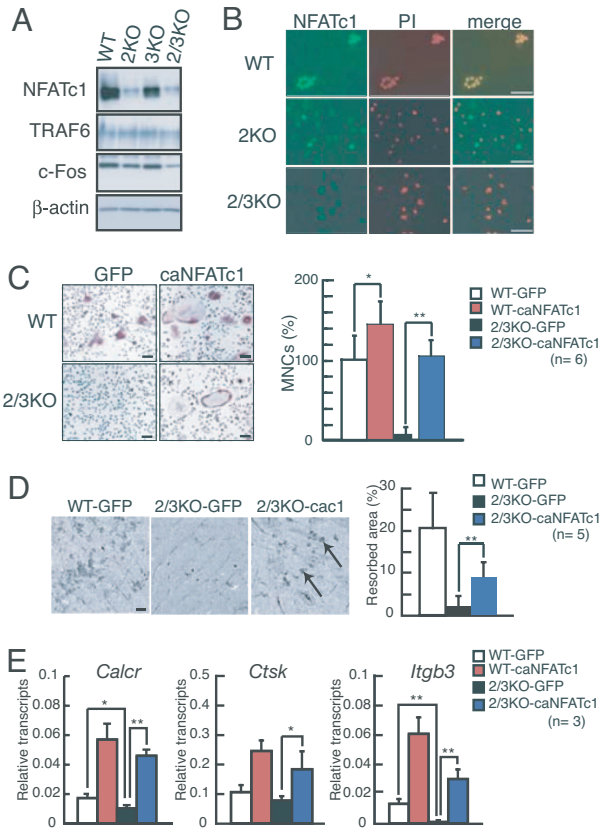

Fig. 2. NFATc1 rescues defects in RANKL/M-CSF-induced osteoclastogenesis of IP_3R2-deficient BMMs. (*A*) Expression levels of key proteins in osteoclast differentiation (TRAF6, c-Fos, and NFATc1) in BMMs treated with RANKL/M-CSF for 4 days. (*B*) Immunostaining of NFATc1 in WT, IP_3R2 KO, and $IP_3R2/3$ KO BMMs exposed to RANKL/M-CSF for 72 h. Nuclei were stained with propidium iodide (PI). (Scale bars, 50 μm.) (*C*) TRAP staining of WT (*Upper*) and $IP_3R2/3$ KO (*Lower*) BMMs infected with retroviruses encoding either the constitutively active form of NFATc1 plus GFP (caNFATc1) or GFP alone (GFP). (Scale bars, 100 μm.) The relative percentage of TRAP-positive multinuclear osteoclasts (MNCs) is shown in the *Right* ($n = 6$). (*D*) Bone resorption assay. Arrows in *Right* show bone resorption pits. (Scale bars, 100 μm.) (*E*) Transcripts of osteoclast terminal differentiation markers (*Calcr*, *Ctsk*, and *Itgkb3*) in RANKL-treated BMMs overexpressing caNFATc1 were analyzed by real-time PCR and normalized to *Gapdh* levels. *, $P < 0.05$; **, $P < 0.01$. All experiments were performed at least three times, and representative data are shown.

proteins from RANKL/M-CSF-treated cells with antibodies specific for each IP_3R subtype revealed that IP_3R2 and IP_3R3 but not IP_3R1 (data not shown) are expressed in WT osteoclasts (Fig. 1*B*). Furthermore, the overall IP_3R expression level detected by pan-IP_3R antibodies recognizing all three subtypes at similar levels (21) was significantly decreased in osteoclast lysates from IP_3R2 KO mice but only modestly reduced in lysates from IP_3R3 KO mice and was completely absent in lysates from $IP_3R2/3$ KO mice (Fig. 1*B Top*), indicating that IP_3R2 is the predominant form expressed in osteoclasts.

Because sustained Ca^{2+} oscillation induced by RANKL is reportedly necessary for osteoclastogenesis (14), we next investigated intracellular Ca^{2+} dynamics in IP_3R2 KO and $IP_3R2/3$ KO BMMs in response to RANKL stimulation. As reported, sustained Ca^{2+} oscillation was clearly observed in WT cells after RANKL stimulation; however, Ca^{2+} oscillation was abolished in BMMs from IP_3R2 KO and $IP_3R2/3$ KO mice (Fig. 1*C*). These results indicate that IP_3R2 is predominantly expressed in osteoclasts and is critical to generate recombinant RANKL/M-CSF-induced Ca^{2+} oscillation and subsequent osteoclastogenesis.

RANKL/M-CSF-Induced NFATc1 Activation Is Abolished in BMMs Lacking IP_3R2. We next examined NFATc1 expression in BMMs lacking IP_3Rs and treated with RANKL/M-CSF for 4 days. As shown in Fig. 2*A Top*, NFATc1 expression levels in BMMs derived from IP_3R2 KO or $IP_3R2/3$ KO mice were dramatically decreased. In contrast, the expression levels of TRAF6 in IP_3R2 KO or $IP_3R2/3$ KO cells were nearly equal to, and that of c-Fos were slightly decreased compared with, WT osteoclasts (Fig. 2*A*). In addition, consistent with decreased NFATc1 expression seen in BMMs from IP_3R2 KO and $IP_3R2/3$ KO mice (Fig. 2*A*), NFATc1 immunoreactivity was barely detectable in IP_3R2 KO cells and completely absent in $IP_3R2/3$ KO cells (Fig. 2*B Middle* and *Bottom*). Together with the finding that IP_3R2 is required to generate Ca^{2+} oscillation activating calcineurin, these results suggest that a defect in NFATc1 activation accounts for impaired RANKL/M-CSF-induced osteoclastogenesis seen in BMMs lacking IP_3R2 (Fig. 1*A*). Indeed, when we ectopically expressed a constitutively active form of NFATc1 (caNFATc1) in $IP_3R2/3$ KO BMMs using retroviral gene transfer, infected $IP_3R2/3$ KO BMMs differentiated into TRAP-positive multinuclear osteoclasts similar to WT BMMs after RANKL/M-CSF stimulation (Fig. 2*C*). $IP_3R2/3$ KO osteoclasts overexpressing caNFATc1 were mature and functional, because they resorbed bone surface

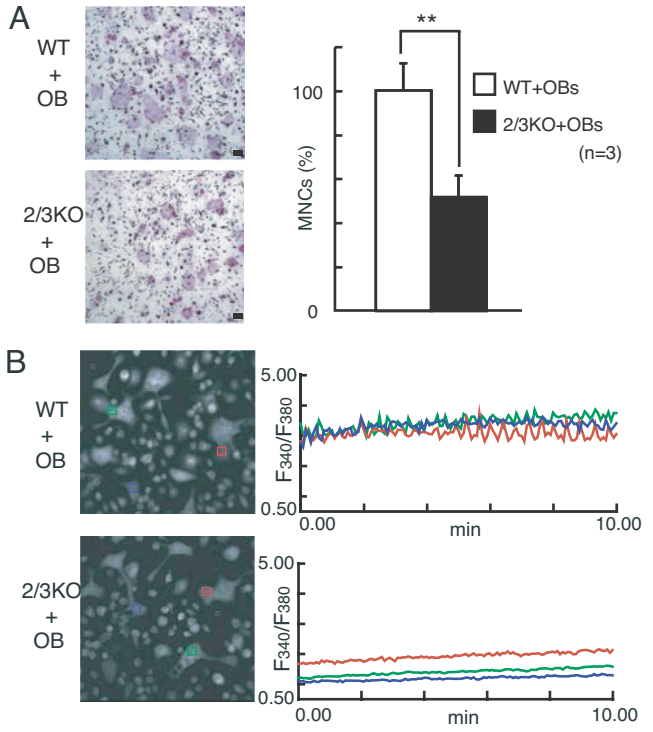

Fig. 3. Ca^{2+} oscillation-independent osteoclastogenesis induced by osteoblasts. (*A*) BMMs from IP_3R2 KO and $IP_3R2/3$ KO mice can differentiate into multinuclear osteoclasts when cocultured with calvarial primary osteoblasts (OB) (TRAP staining). (*Right Upper*) The relative percentage of TRAP-positive MNCs seen during coculture with calvarial primary osteoblasts ($n = 3$). (Scale bars, 100 μm.) **, $P < 0.01$. (*B*) Ca^{2+} oscillation in multinuclear osteoclasts cocultured with osteoblasts. *Left* show fura-2 images of recorded cells, and *Right* show traces of change in the fura-2 fluorescence ratio in single cells cocultured with OB for 6 days. Each colored box represents the area from which the time-course plot was calculated. All experiments were performed at least three times, and representative data are shown.

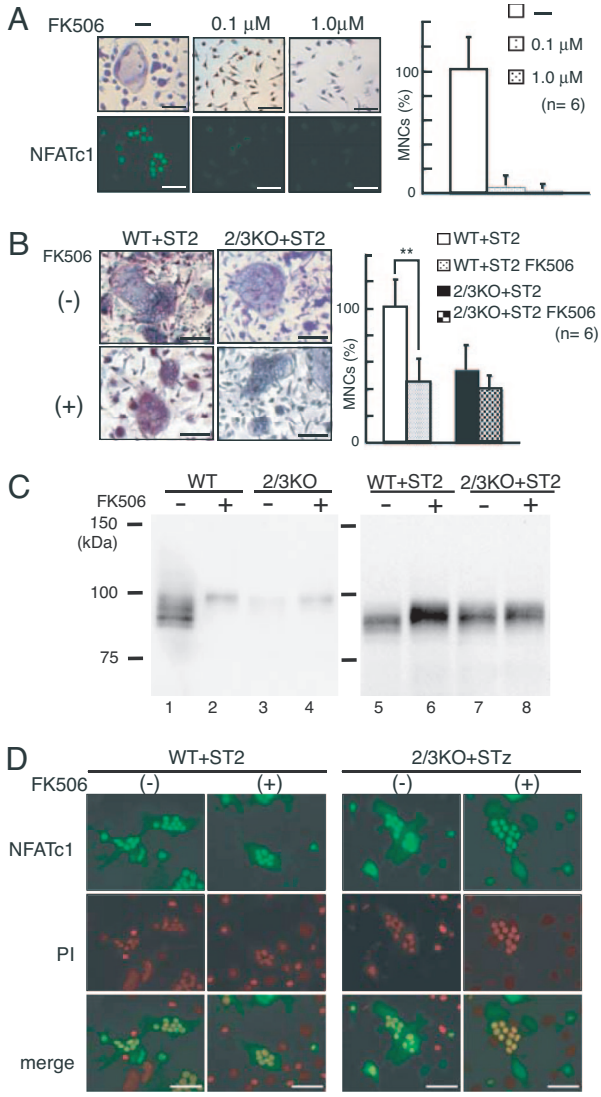

Fig. 4. Effect of the calcineurin inhibitor FK506 on RANKL/M-CSF-induced or osteoblast-induced osteoclastogenesis and on NFATc1 induction. (*A*) Dose-dependent suppression of RANKL/M-CSF-induced osteoclastogenesis by FK506. *Upper* and *Lower* show osteoclast formation visualized by TRAP staining and NFAT immunostaining (green), respectively. (Scale bars, 50 μm.) *Right* shows the relative percentage of TRAP-positive MNCs ($n = 6$). (*B*) Effect of FK506 on osteoblast-induced osteoclastogenesis. BMMs from WT or $IP_3R2/3$ KO mice were cocultured with ST2 cells in the absence (*Left Upper*) or presence (*Left Lower*) of 1.0 μM FK506. (Scale bars, 50 μm.) *Right* shows the relative percentage of TRAP-positive MNCs ($n = 6$). **, $P < 0.01$. (*C*) NFATc1 expression in RANKL/M-CSF-induced osteoclasts (*Left*) and osteoblast-induced osteoclasts (*Right*) in the absence (−) or presence (+) of FK506. (*D*) Calcineurin-independent NFAT activation in WT and $IP_3R2/3$ KO osteoclasts cocultured with ST2 cells. *Top* and *Middle* show NFAT signals (green) and PI staining (red), respectively. *Bottom* shows merged images of NFAT and PI signals. (Scale bars, 50 μm.) Experiments were performed at least three times, and representative data are shown.

(Fig. 2*D*) and expressed terminal osteoclast markers (Fig. 2*E*). In contrast, although the expression levels of c-Fos in IP_3R2 KO or $IP_3R2/3$ KO cells were slightly decreased compared with WT osteoclasts (Fig. 2*A*), we could not rescue recombinant RANKL-induced osteoclastogenesis of $IP_3R2/3$ KO cells by overexpressing c-Fos (data not shown). These results indicate that impaired NFATc1 activation is the primary cause of defects in osteoclastogenesis seen in IP_3R2 KO and $IP_3R2/3$ KO BMMs.

Osteoblasts Induce Osteoclastogenesis of BMMs Lacking IP_3R2 in a Ca^{2+} Oscillation/Calcineurin-Independent Manner. Because osteoblasts regulate the differentiation and function of osteoclasts by producing M-CSF, RANKL, and other cytokines (1) and membrane-bound molecules *in vivo* (26), we examined osteoclastogenesis induced by coculture with osteoblasts. Interestingly, we found that $IP_3R2/3$ KO BMMs underwent osteoclast differentiation when cocultured with primary calvarial osteoblasts (Fig. 3*A*) or ST2 cells (Fig. 4*B Upper*), although the numbers of multinuclear osteoclasts were almost half of those seen in WT controls. Interestingly, we did not detect Ca^{2+} oscillations in multinuclear $IP_3R2/3$ KO osteoclasts generated by coculture with primary osteoblasts (Fig. 3*B*). Therefore, although IP_3R2-mediated Ca^{2+} oscillation is required for efficient osteoclastogenesis, these results suggest that osteoblasts rescue deficiencies in osteoclastogenesis in IP_3R2 KO BMMs through Ca^{2+} oscillation/calcineurin-independent mechanism(s).

To confirm the existence of Ca^{2+} oscillation/calcineurin-independent signaling for osteoclastogenesis in a coculture system, we investigated the effect of FK506, a specific calcineurin inhibitor, on osteoblast-induced osteoclastogenesis. As reported (14), FK506 abolished multinuclear osteoclasts and nuclear NFATc1 localization during the course of recombinant RANKL/M-CSF-induced osteoclast differentiation from WT BMMs at 1.0 μM (Fig. 4*A*). However, in the case of coculturing with ST2 cells, FK506 (1.0 μM) treatment decreased the number of multinuclear osteoclasts by approximately half but did not

CELL BIOLOGY

abolish WT osteoclast differentiation (Fig. 4*B*). This suggests that both Ca^{2+} oscillation/calcineurin-dependent and -independent signal transduction pathways are activated during osteoblast-induced osteoclastogenesis, and that residual osteoclastogenesis seen in the presence of FK506 is induced by the Ca^{2+} oscillation/calcineurin-independent pathway. Consistently, FK506 treatment did not significantly affect osteoclastogenesis by $IP_3R2/3$ KO BMMs in a coculture system that relies on Ca^{2+} oscillation-independent osteoclastogenesis (Fig. 4*B*).

We also examined the expression level and cellular localization of NFATc1 in FK506-treated multinuclear osteoclasts. In recombinant RANKL/M-CSF-induced osteoclastogenesis, FK506 application severely decreased NFATc1 expression and reduced the mobility of NFATc1 on SDS/PAGE at 100 kDa in WT cells (Fig. 4*C*, lanes 1 and 2). $IP_3R2/3$ KO cells did not show strong NFATc1 expression, and only a faint band migrating at 100 kDa was observed in recombinant RANKL/M-CSF-treated cells (Fig. 4*C*, lane 3). By contrast, under coculture conditions, FK506 treatment slightly reduced NFATc1 mobility but did not apparently affect its expression level in cocultured WT cells in which both Ca^{2+} oscillation-dependent and -independent NFATc1 activation were functioning (Fig. 4*C*, lanes 5 and 6). In addition, a clear NFATc1 band smaller than 100 kDa was detected in cocultured $IP_3R2/3$ KO cells. Interestingly, NFATc1 mobility on SDS/PAGE in FK506-treated cocultured WT cells was almost the same as that in nontreated cocultured $IP_3R2/3$ KO cells (Fig. 4*C*, lanes 6 and 7). Furthermore, the expression and mobility of NFATc1 in $IP_3R2/3$ KO cells in coculture were not affected by FK506 treatment (Fig. 4*C*, lanes 7 and 8). Immunocytochemical studies revealed strong nuclear NFATc1 signals in both WT and $IP_3R2/3$ KO multinuclear osteoclasts, even in the presence of FK506 (Fig. 4*D*). Taken together, these results suggest that a Ca^{2+} oscillation/calcineurin-independent NFATc1 activation mechanism is activated upon osteoblast-induced osteoclastogenesis, and that some modification, such as the phosphorylation, of NFATc1 activated by the Ca^{2+} oscillation-independent signal pathway during osteoblast-induced osteoclastogenesis, clearly differs from that seen during RANKL/MCSF-induced osteoclastogenesis.

Ca^{2+} Oscillation-Independent Osteoclastogenesis Occurs *in Vivo*. Finally, we analyzed bone phenotypes of IP_3R2-deficient mice to confirm that Ca^{2+} oscillation/calcineurin-independent osteoclastogenesis occurs *in vivo*. Consistent with results seen in the coculture system described above, IP_3R2 KO and $IP_3R2/3$ KO mice showed TRAP-positive multinuclear osteoclasts in femurs (Fig. 5*A*), and osteoclast numbers and bone volume seen in $IP_3R2/3$ KO mice at P17 did not differ significantly from those seen in WT mice (Fig. 5*B*). Even at the adult stage, the bone density of IP_3R2 KO is not increased compared with WT mice [supporting information (SI) Fig. S1*A*], and $IP_3R2/3$ KO mice rather showed decreased bone density probably due to the malnutrition caused by indigestion and the resulting decreased of body weight (ref. 25 and Fig. S1*B*). These results strongly support the idea that osteoblasts promote osteoclastogenesis through NFATc1 activation in both a Ca^{2+} oscillation/calcineurin-dependent and -independent manner (Fig. 5*C*).

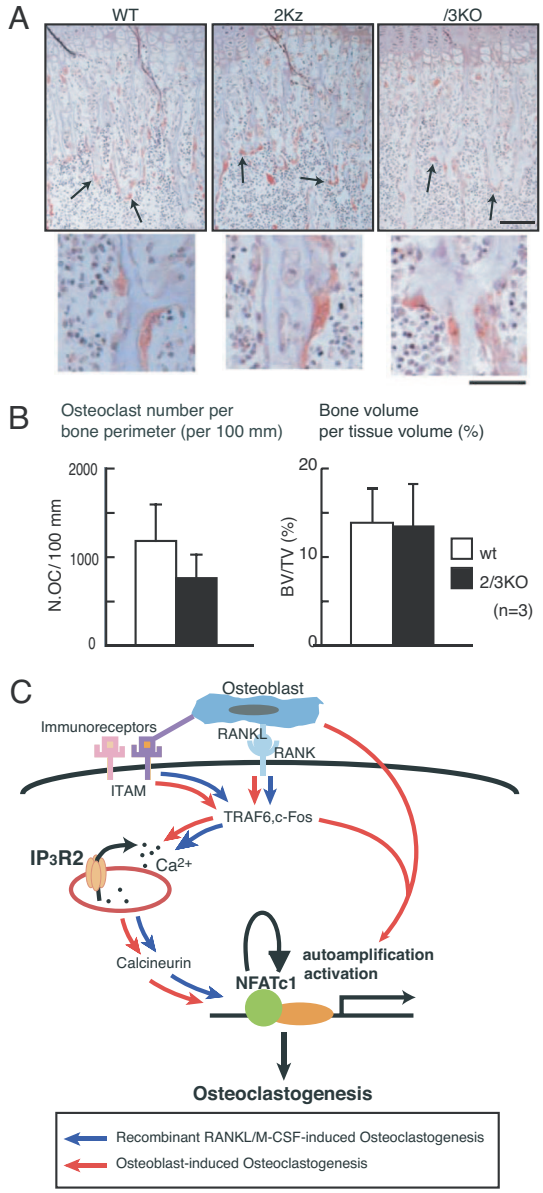

Fig. 5. Bone phenotype of IP_3R2-deficient mice. (*A*) Histological appearance of the femoral metaphysis of 17-day-old WT, IP_3R2 KO, and $IP_3R2/3$ KO mice (TRAP staining, $n = 3$). [Scale bars, 100 μm (*Upper*) and 50 μm (*Lower*).] Arrows in *Upper* show TRAP-positive multinuclear osteoclasts. (*B*) Osteoclast numbers and bone volume in primary spongiosa area of a femur of 17-day-old WT and $IP_3R2/3$ KO mice ($n = 3$). (*C*) Schematic model of recombinant RANKL/M-CSF- and osteoblast-induced osteoclastogenesis. In recombinant RANKL/M-CSF-induced osteoclastogenesis, NFATc1 is activated by the Ca^{2+} oscillation/calcineurin-dependent pathway alone, with IP_3R2 acting as a key molecule. In osteoblast-induced osteoclastogenesis, NFATc1 is activated by both Ca^{2+} oscillation/calcium-dependent and -independent pathways.

Discussion

Although it is well known that Ca^{2+} oscillation frequency is important for NFAT activation (27) and RANKL-induced osteoclastogenesis (14, 28), how Ca^{2+} oscillation is established during osteoclastogenesis remains unknown. In this study, using BMMs from mice lacking various IP_3Rs, we showed that IP_3R2 critically determines generation of Ca^{2+} oscillation and subsequent NFATc1 activation in RANKL/M-CSF-induced osteoclastogenesis. By contrast, although we found that IP_3R3 is expressed in osteoclasts, we did not observe changes in RANKL-induced Ca^{2+} oscillation (data not shown) or osteoclastogenesis in IP_3R3 KO BMMs (Fig. 1*A*). These results may be due to the predominant expression of IP_3R2 among the three IP_3R subtypes in BMMs (Fig. 1*B*) and may reflect previous findings that IP_3R2, rather than IP_3R3, contributes to the establishment of sustained Ca^{2+} oscillation (20, 21). However, because we detected faint nuclear NFATc1 immunosignaling in a small population of IP_3R2 KO BMMs after RANKL stimulation (Fig. 2*B*), IP_3R3 may contribute in part to NFATc1 activation via a transient Ca^{2+} increase not detected under our experimental

conditions. It should be noted that $IP_3R2/3$ KO BMMs showed lower basal levels of intracellular Ca^{2+} than did WT BMMs (Figs. 1*C* and 3*B*). Depletion of extracellular Ca^{2+} from WT BMMs reduced not only Ca^{2+} oscillation but also basal Ca^{2+} levels to those observed in BMMs lacking $IP_3R2/3$ (Fig. S2). This observation suggests that IP_3Rs are necessary for Ca^{2+} influx and to maintain Ca^{2+} oscillation over the relatively high cytosolic basal Ca^{2+} level.

An important finding reported here is the observation of Ca^{2+} oscillation/calcineurin-independent osteoclastogenesis. It is clear that IP_3R deficiency impairs osteoclast differentiation, because RANKL-induced Ca^{2+} oscillation is essential for osteoclastogenesis. However, we show that IP_3R2 KO and $IP_3R2/3$ KO mice exhibit TRAP-positive multinuclear osteoclasts in femurs, and that osteoblasts can induce $IP_3R2/3$ KO osteoclastogenesis without detectable Ca^{2+} oscillation in osteoclasts. We also demonstrate that FK506 treatment of WT cells decreases the number of osteoblast-induced multinuclear osteoclasts only by half and does not affect $IP_3R2/3$ KO cells, which lack the Ca^{2+} oscillation/calcineurin-dependent pathway for osteoclast differentiation (Fig. 4*B*). Because the mobility of NFATc1 in WT osteoclasts cocultured with osteoblasts was reduced by 1.0 μM FK506 (Fig. 4*C Right*, lanes 5 and 6), 1.0 μM FK506 likely inhibited Ca^{2+}/calcineurin-mediated NFATc1 dephosphorylation even in the coculture system. These results support our hypothesis that osteoblasts can induce Ca^{2+} oscillation/calcineurin-independent osteoclastogenesis.

An intense nuclear NFATc1 signal was observed in $IP_3R2/3$ KO osteoclasts during osteoblast-induced Ca^{2+} oscillation/calcineurin-independent osteoclastogenesis. It is not known how NFATc1 is activated intercellularly by osteoblasts in a Ca^{2+} oscillation/calcineurin-independent manner. It is known that NFATc1 activity and translocation are controlled by its phosphorylation status, which in turn is regulated by phosphatases and serine/threonine kinases such as GSK3β, PKA, casein kinase I, and DYRK1 (29–31). We observed a subtle mobility shift of NFATc1 on SDS/PAGE between recombinant RANKL/M-CSF-induced and osteoblast-induced osteoclastogenesis: NFATc1 from osteoclasts cocultured with ST2 cells migrated more slowly than NFATc1 in RANKL/M-CSF-treated cells but faster than highly phosphorylated NFATc1 in FK506-treated cells (Fig. 4*C*, lanes 1, 2, and 5). Thus, we are currently analyzing the difference between recombinant RANKL/M-CSF-induced osteoclastogenesis and osteoblast-induced osteoclastogenesis in terms of NFATc1 phosphorylation status.

In summary, the findings presented here further our understanding of the molecular mechanisms underlying osteoclast differentiation. We show that IP_3R2 is necessary for RANKL-induced Ca^{2+} oscillation and efficient NFATc1 activation. We also find that NFATc1 is activated by both Ca^{2+} oscillation/calcineurin-dependent and -independent signal pathways *in vivo*, and that the Ca^{2+} oscillation-independent pathway depends completely on osteoblasts and is not activated during RANKL/M-CSF-induced osteoclastogenesis. It is known that treatment with immunosuppressants leads to bone loss (32). Our findings of immunosuppressant-resistant osteoclastogenesis *in vivo* would partially explain this phenomenon, as well as defects in osteoblast function (33). Further analysis of Ca^{2+} oscillation-independent osteoclastogenesis should reveal the precise molecular mechanisms of osteoclastogenesis *in vivo*, leading to development of new therapies for skeletal disease.

Materials and Methods

Mice and Bone Analysis. Generation of IP_3R1 KO, IP_3R2 KO, IP_3R3 KO, and $IP_3R2/3$ KO mice has been described (24, 25). Histological experiments were performed as described (14). Animals were ethically treated according to the instructions for animal care and use of the Institute of Medical Science, University of Tokyo, and RIKEN Brain Science Institute.

***In Vitro* Osteoclastogenesis.** Nonadherent bone marrow cells derived from mice were seeded (2×10^5 cells per well in a 24-well plate) and cultured in a α-MEM (GIBCO-BRL) with 10% FBS (JRH Biosciences) containing 10 ng/ml M-CSF (R&D Systems). After 3 days, adherent cells were used as BMMs. These osteoclast progenitor cells were further cultured in the presence of 100 ng/ml soluble RANKL (PeproTech) and 10 ng/ml M-CSF to generate osteoclasts. Reagents were used at these concentration unless otherwise indicated. To analyze the effect of FK506 (Calbiochem and Fujisawa Pharmaceutical) on osteoclastogenesis, FK506 was added at the same time as RANKL. Four days later, TRAP-positive multinuclear cells (more than three nuclei) were counted. ST2 cells were described in ref. 34. For coculture with primary osteoblasts or ST2 cells, BMMs were seeded at 6×10^5 cells per cm^2 with $6 \times 10^4/cm^2$ ST2 cells and cultured with 10^{-8} M 1, 25-dihydroxyvitamin D_3 for 4–5 days. In the case of coculture with primary osteoblasts for Ca^{2+} imaging, bone marrow cells were cultured in α-MEM with 10% FBS containing 50 μg/ml L-ascorbic acid (Sigma), 10 mM β-glycerophosphate, 10 ng/ml M-CSF, and 100 ng/ml soluble RANKL for 6 days.

Immunoblotting. Differentiated osteoclasts were washed with PBS, lysed with sample buffer (125 mM Tris·HCl, pH 6.8; 20% glycerol; 4.0% SDS; 10% 2-mercaptoethanol; 0.1% bromophenol blue) and boiled 3 min. Primary antibodies used were anti-IP_3R1 mAb 18A10 (35), anti-IP_3R2 mAb KM1083, anti-IP_3R3 mAb KM1082 (36), anti-pan-IP_3R polyclonal antibody (21), anti-NFATc1 mAb 7A6 (Santa Cruz Biotechnology), anti-TRAF6 polyclonal antibody (H-274, Santa Cruz Biotechnology), anti-c-Fos polyclonal antibody (Santa Cruz Biotechnology), and anti-β-actin mAb AC-15 (Sigma).

Immunocytochemistry. BMMs grown on glass coverslips were stimulated with RANKL/M-CSF for the indicated periods, washed once with PBS, fixed in 4.0% paraformaldehyde/PBS for 10 min, and treated with 0.2% Triton X-100/PBS for 5 min. Cells were sequentially incubated with 1.0% skim milk/PBS for 1 h and 1.0 μg/ml anti-NFATc1 mAb 7A6 (Santa Cruz Biotechnology) for 1 h at room temperature (RT). After washing with PBS, cells were stained with Alexa Fluor 488-conjugated goat anti-mouse IgG or Alexa Fluor 594-conjugated goat anti-mouse IgG (Molecular Probes) for 1 h at RT. After washing, coverslips were mounted with Vectashield (Vector Laboratories) and observed under a IX-70 confocal fluorescence microscope (Olympus).

Intracellular Ca^{2+} Imaging. Cells plated on 3.5-cm poly-L-lysine-coated glass bottom dishes (Matsunami) were loaded with 5 μM Fura-2/AM (Dojindo) for 30 min at RT in loading solution: 115 mM NaCl, 5.4 mM KCl, 1 mM $MgCl_2$, 2 mM $CaCl_2$, 20 mM Hepes, and 10 mM glucose, pH 7.42. Fura-2 fluorescent images were analyzed using an inverted microscope (ECLIPSE TE300, Nikon) and a video image analysis system (Argus-50/CA, Hamamatsu Photonics) with excitation filters at 340 $\pm$ 10 and 380 $\pm$ 10 nm, a dichroic beam splitter at 400 nm, and a bandpass emission filter at 510–550 nm. The recording solution contained: 115 mM NaCl, 5.4 mM KCl, 1 mM $MgCl_2$, 2 mM $CaCl_2$, 20 mM Hepes, and 10 mM glucose, pH 7.42.

Bone Resorption Assay. Infected cells were cultured on bone slices prepared as described (26) for 7 days in the presence of RANKL/M-CSF. Bone slice surfaces were visualized by backscattered electron imaging, as described (37).

Real-Time RT-PCR. Total RNA was extracted from osteoclasts infected with virus expressing GFP or GFP + caNFATc1. First-strand cDNA was produced from total RNA using Reverse Transcriptase SuperScript II (Invitrogen) and oligonucleotide (dT) primers. Calcitonin receptor (*Calcr*) and Cathepsin K (*Ctsk*) transcripts were quantified on an ABI PRISM 7000 (Applied Biosystems) using SYBR green and Integrin β3 (*Itgb3*, Assay ID, Mm00443980_m1), and Gapdh transcripts were quantified using primer/probe kit (TaqMan Gene Expression Assays, Applied Biosystems). *Calcr*, *Ctsk*, and *Intgb3* transcripts were normalized to glyceraldehyde-3-phosphate dehydrogenase (*Gapdh*) transcripts. Primer sequences were: *Calcr*-1376F, 5′-TTACCGACGAGCAACGCCTA-3′; *Calcr*-1584R, 5′-CACGCGGACAATGTTGAGAA-3′; *Ctsk*-F, 5′-ACGGGACTCAGAATACCTCCCT-3′; and *Ctsk*-R, 5′-CTCTCTGTACCCTCTGCATTTAGC-3.

Statistical Analysis. Statistical analysis was performed by using Student's *t* test (*, $P < 0.05$; **, $P < 0.01$). All data are presented as means $\pm$ SD.

For the analysis of bone density, see *SI Materials and Methods*.

ACKNOWLEDGMENTS. We thank Dr. Neil A. Clipstone (Northwestern University, Chicago) for the pMSCV-GFP and pMSCV-caNFATc1-IRES-GFP vector plasmids. We also thank Dr. S. Iwai (University of Tokyo, Tokyo) for technical help; H. Murayama (Kureha Chemical Industry, Japan) for excellent technical help and discussion; Dr. H. Amano (Showa University, Japan) for help with backscattered electron imag-

ing; all members of our laboratories, especially T. Inoue, for critical reading of the manuscript and providing TI Workbench software; K. Nakamura and N. Ogawa for excellent technical help; and A. Terauchi, N. Matsumoto, and E. Ebisui for supplying valuable materials. This work was supported by a grant from the Japan Science and Technology Agency, by grants-in-aid (to K. Mikoshiba, C. Hisatsune, and Y. Kuroda), and by the 21st Century COE Program, Center for Integrated Brain Medical Science, from the Ministry of Education, Culture, Sports, Science and Technology, Japan.

1. Boyle WJ, Simonet WS, Lacey DL (2003) Osteoclast differentiation and activation. *Nature* 423:337–342.
2. Karsenty G, Wagner EF (2002) Reaching a genetic and molecular understanding of skeletal development. *Dev Cell* 2:389–406.
3. Yasuda H, *et al.* (1998) Osteoclast differentiation factor is a ligand for osteoprotegerin/osteoclastogenesis-inhibitory factor and is identical to TRANCE/RANKL. *Proc Natl Acad Sci USA* 95:3597–3602.
4. Lacey DL, *et al.* (1998) Osteoprotegerin ligand is a cytokine that regulates osteoclast differentiation and activation. *Cell* 93:165–176.
5. Kong YY, *et al.* (1999) OPGL is a key regulator of osteoclastogenesis, lymphocyte development and lymph-node organogenesis. *Nature* 397:315–323.
6. Hsu H, *et al.* (1999) Tumor necrosis factor receptor family member RANK mediates osteoclast differentiation and activation induced by osteoprotegerin ligand. *Proc Natl Acad Sci USA* 96:3540–3545.
7. Yoshida H, *et al.* (1990) The murine mutation osteopetrosis is in the coding region of the macrophage colony stimulating factor gene. *Nature* 345:442–444.
8. Lagasse E, Weissman IL (1997) Enforced expression of Bcl-2 in monocytes rescues macrophages and partially reverses osteopetrosis in op/op mice. *Cell* 89:1021–1031.
9. Naito A, *et al.* (1999) Severe osteopetrosis, defective interleukin-1 signalling and lymph node organogenesis in TRAF6-deficient mice. *Genes Cells* 4:353–362.
10. Wong BR, *et al.* (1998) The TRAF family of signal transducers mediates NF-kappaB activation by the TRANCE receptor. *J Biol Chem* 273:28355–28359.
11. Kobayashi N, *et al.* (2001) Segregation of TRAF6-mediated signaling pathways clarifies its role in osteoclastogenesis. *EMBO J* 20:1271–1280.
12. Matsuo K, *et al.* (2000) Fosl1 is a transcriptional target of c-Fos during osteoclast differentiation. *Nat Genet* 24:184–187.
13. Wagner EF, Karsenty G (2001) Genetic control of skeletal development. *Curr Opin Genet Dev* 11:527–532.
14. Takayanagi H, *et al.* (2002) Induction and activation of the transcription factor NFATc1 (NFAT2) integrate RANKL signaling in terminal differentiation of osteoclasts. *Dev Cell* 3:889–901.
15. Crabtree GR (1999) Generic signals and specific outcomes: signaling through Ca2+, calcineurin, and NF-AT. *Cell* 96:611–614.
16. Graef IA, Chen F, Crabtree GR (2001) NFAT signaling in vertebrate development. *Curr Opin Genet Dev* 11:505–512.
17. Rusnak F, Mertz P (2000) Calcineurin: Form and function. *Physiol Rev* 80:1483–1521.
18. Higo T, *et al.* (2005) Subtype-specific and ER lumenal environment-dependent regulation of inositol 1,4,5-trisphosphate receptor type 1 by ERp44. *Cell* 120:85–98.
19. Ando H, *et al.* (2006) IRBIT suppresses IP3 receptor activity by competing with IP3 for the common binding site on the IP3 receptor. *Mol Cell* 22:795–806.
20. Miyakawa T, *et al.* (1999) Encoding of Ca2+ signals by differential expression of IP3 receptor subtypes. *EMBO J* 18:1303–1308.
21. Hattori M, *et al.* (2004) Distinct roles of inositol 1,4,5-trisphosphate receptor types 1 and 3 in Ca2+ signaling. *J Biol Chem* 279:11967–11975.
22. Sugawara H, Kurosaki M, Takata M, Kurosaki T (1997) Genetic evidence for involvement of type 1, type 2 and type 3 inositol 1,4,5-trisphosphate receptors in signal transduction through the B-cell antigen receptor. *EMBO J* 16:3078–3088.
23. Groth RD, Mermelstein PG (2003) Brain-derived neurotrophic factor activation of NFAT (nuclear factor of activated T cells)-dependent transcription: A role for the transcription factor NFATc4 in neurotrophin-mediated gene expression. *J Neurosci* 23:8125–8134.
24. Matsumoto M, *et al.* (1996) Ataxia and epileptic seizures in mice lacking type 1 inositol 1,4,5-trisphosphate receptor. *Nature* 379:168–171.
25. Futatsugi A, *et al.* (2005) IP3 receptor types 2 and 3 mediate exocrine secretion underlying energy metabolism. *Science* 309:2232–2234.
26. Zhao C, *et al.* (2006) Bidirectional ephrinB2-EphB4 signaling controls bone homeostasis. *Cell Metab* 4:111–121.
27. Dolmetsch RE, Xu K, Lewis RS (1998) Calcium oscillations increase the efficiency and specificity of gene expression. *Nature* 392:933–936.
28. Koga T, *et al.* (2004) Costimulatory signals mediated by the ITAM motif cooperate with RANKL for bone homeostasis. *Nature* 428:758–763.
29. Rao A, Luo C, Hogan PG (1997) Transcription factors of the NFAT family: regulation and function. *Annu Rev Immunol* 15:707–747.
30. Gwack Y, *et al.* (2006) A genome-wide *Drosophila* RNAi screen identifies DYRK-family kinases as regulators of NFAT. *Nature* 441:646–650.
31. Arron JR, *et al.* (2006) NFAT dysregulation by increased dosage of DSCR1 and DYRK1A on chromosome 21. *Nature* 441:595–600.
32. Cvetkovic M, *et al.* (1994) The deleterious effects of long-term cyclosporine A, cyclosporine G, and FK506 on bone mineral metabolism *in vivo*. *Transplantation* 57:1231–1237.
33. Koga T, *et al.* (2005) NFAT and Osterix cooperatively regulate bone formation. *Nat Med* 11:880–885.
34. Lean JM, *et al.* (2000) Osteoclast lineage commitment of bone marrow precursors through expression of membrane-bound TRANCE. *Bone* 27:29–40.
35. Maeda N, Niinobe M, Nakahira K, Mikoshiba K (1988) Purification and characterization of P400 protein, a glycoprotein characteristic of Purkinje cell, from mouse cerebellum. *J Neurochem* 51:1724–1730.
36. Sugiyama T, *et al.* (1994) Monoclonal antibodies distinctively recognizing the subtypes of inositol 1,4,5-trisphosphate receptor: Application to the studies on inflammatory cells. *FEBS Lett* 354:149–154.
37. Matsuo K, *et al.* (2004) Nuclear factor of activated T-cells (NFAT) rescues osteoclastogenesis in precursors lacking c-Fos. *J Biol Chem* 279:26475–26480.